Creep behaviour of bischofite, carnallite and mixed bischofite-carnallite-halite salt rock at *in situ* conditions

N. Muhammad[1], J.H.P. de Bresser[2], C.J. Peach[2], C.J. Spiers[2]*

[1]Center for Advanced Studies in Physics, GC University Lahore, Pakistan; [2]Experimental Rock Deformation Laboratory, Department of Earth Sciences, Utrecht University, the Netherlands

** nawazmuhammad@gcu.edu.pk*

ABSTRACT: To accurately predict cavern convergence and subsidence caused by solution mining of K- and Mg-bearing salt bodies, a good understanding of the creep behaviour of bischofite, carnallite and mixed salts rocks is required. We studied the mechanical properties of these materials aiming to produce flow laws that can be applied at *in situ* conditions. We performed triaxial deformation experiments on natural polycrystalline samples of bischofite, carnallite (starting grain size ~5 mm), and their mixtures with halite, at *in situ* PT conditions of 40 MPa and 70 °C. All deformation tests were done in strain rate stepping mode, with intervening stress relaxation to reach low strain rates. We found that carnallite is 4-5 times stronger than bischofite, and that bischofite-carnallite-halite mixtures are stronger than carnallite. The constant strain rate parts of the multistep experiments allowed dislocation creep laws to be defined for bischofite and carnallite at relatively high stress, with a power law stress exponent n~5. During stress relaxation, n changes to ~1 at a strain rate of ~10^{-9} s^{-1}. This is interpreted as reflecting a change from dislocation creep at the faster strain rates to solution-precipitation behaviour at slow strain rate, mediated by changing grain size.

1 Introduction

The salt deposits at Veendam (northern part of the Netherlands) are mainly composed of the evaporites bischofite, carnallite and halite in the form of layers and mixtures, with sulphates in minor quantities. In order to solution mine the caverns, it is important to know the rheology of the different salts at *in situ* conditions, so that the rate of inflow into the caverns as well as surface subsidence can be predicted. The strain rate of such salts in underground mines is normally in the range of 10^{-8} to 10^{-15} s^{-1} (Heard 1972; Van Eekelen et al. 1981; Jackson & Talbot 1986) which is a rate that cannot be achieved easily in laboratory scale experiments. However, laboratory experiments can be used to define a flow law that allows extrapolation to *in situ* conditions. In order to perform such extrapolation in a reliable manner, good understanding of the deformation mechanism of the material is needed, so that the characteristics of the flow law can be related to the microphysical mechanism controlling creep.

Van Eekelen et al. (1981) and Urai (1983) have tested the creep behaviour of bischofite at a fixed confining pressure of 28 MPa, in the temperature range of 40-80 °C, with varying water content including dry samples. The authors suggested that a conventional power law of the type $\dot{\varepsilon} \sim \sigma^n$, relating strain rate $\dot{\varepsilon}$ to stress σ, can be used to describe the flow behaviour of bischofite, as long as two regimes were defined, one at low and one at relatively high differential stress. The flow laws of the two regimes show different values of the power law stress exponent n, namely 1.5 and 4 for the low and high stress regime, respectively. However, the nature of the two regimes was not fully understood and accordingly, a good basis for establishing the rate of inflow relevant in the case of cavern evolution associated with solution mining is still missing.

The creep properties of dry and wet carnallite have been studied by Urai (1985), by performing triaxial deformation experiments at a temperature of 60 °C, using a range of strain rates and confining pressures. Urai (1985) proposed a conventional power law for steady state creep of wet carnallite with stress exponent n = 4.8±0.1. The strength of carnallite was found to be substantially higher than that of bischofite. It is yet unknown what the rheology of mixtures of

bischofite and carnallite is like, and which of these salts dominates creep in a mixture. Also, halite, both as natural single and poly-crystals and as artificially prepared dense aggregates, has been studied before for its creep properties under dry and wet conditions (Heard 1972; Heard & Ryerson 1986; Wawersik & Zeuch 1986; Urai et al. 1986; Spiers et al. 1990; Senseny et al. 1992; Carter et al. 1993; Spiers & Carter 1998; Ter Heege et al. 2005b; Muhammad et al. 2012). Also, for this material, a conventional power law appears to describe the behaviour well. For wet salt, the proposed stress exponent *n* lies in the range of 4.1 to 5.7, in the temperature range of 23 to 400 °C.

In the current work, we have performed triaxial deformation experiments on polycrystalline natural samples of bischofite, carnallite and their mixture with halite, at *in situ* conditions of confining pressure 40 MPa and at a fixed temperature of 70 °C. All deformation tests were done in strain rate stepping mode, with several steps being followed by stress relaxation (Rutter & Mainprice 1978), with the aim to achieve strain rates as low as ~10^{-9} s^{-1}, approaching the natural strain rates in salt caverns.

2 Method

2.1 Sample preparation

The natural cores of bischofite, carnallite and their mixture with halite (mixture1: halite 65%, carnallite 4%, bischofite 14%, mixture2: halite 30%, carnallite 37%, bischofite 19%), extracted by Nedmag Industries Mining & Manufacturing B.V. during the so-called TR9 drilling project, were provided with 100 mm diameter and 1 m length, along with the description. The cores were first cut down to rectangular rods of about 100 mm length and 50 mm diameter using a hand saw. These rods were then shaped down to samples with the required dimensions of 35 mm diameter and 85 mm (average) length, using SiC papers. Since the salts under investigation are hygroscopic, the samples were prepared in a low humidity room with relative humidity (R.H.) < 15% to control the water content. Natural salts in general are wet (Roedder & Bassett 1981; Urai 1983). In order to create a deliquescence condition in our samples, comparable to that at *in-situ* conditions, the samples were first equilibrated with air with R.H. > 30% (Urai 1985; Christov 2009) and, in parallel, carefully measured for increase in weight by water absorption. This was followed by wrapping up the samples in a double layer of perforated glass fibre sheet (0.3 mm starting thickness) creating an equilibrated humid environment around the sample. These wrapped samples were further sealed in 1.0 mm thick polymer “ethylene propylene diene monomer (EPDM)” jackets to avoid contamination of the samples by the confining medium (silicone oil) used in the deformation apparatus.

2.2 Deformation apparatus

The apparatus used for this study was the so-called “Shuttle Vessel” of the experimental rock deformation (HPT) laboratory at the department of Earth Sciences at Utrecht University. The Shuttle Vessel machine is an internally heated 100 MPa confining pressure vessel mounted on a standard 100 kN Instron 1362 loading frame with an electro-mechanical servo-controlled positioning system. The machine is provided with a (Instron standard, +/-50 mm) linear variable differential transformer (LVDT), but to come to an accurate measurement of the sample deformation, a second LVDT (0-25 mm range, H.F. Jensen, Denmark) was installed at the top of the vessel and near the sample. This was done to reduce the effect of the elastic distortion of the apparatus and measure accurately the shortening of the sample, especially during stress relaxation, where very limited natural strain in the order of 0.001 is to be monitored. Further details can be seen in Muhammad (2015).

2.3 Experiments

In this study, multistep experiments were performed. A typical experiment consisted of a few steps at constant strain rate, in the range 10^{-5} to 10^{-8} s^{-1}, interrupted by periods of stress relaxation. During the constant strain rate part of the test, the sample was deformed until a steady (or near steady) state of stress was reached. This usually required about 2-4% of shortening. Then the piston was arrested and the stress on the sample was allowed to relax until the diminishing force on the sample reached the limits of the load cell resolution. The duration of each relaxation step was a few days. The experiments were performed at 70 °C sample temperature and 40 MPa confining pressure for *in situ* conditions.

2.4 Data acquisition and processing

The data containing pressure, temperature, load, and position (LVDT_1 and 2) were logged throughout the test. The stress on the sample was calculated from the load values by assuming constant volume deformation, correcting the instantaneous change in area value for progressive change in length of the sample. The data acquired during stress relaxation was analysed with a dedicated code to produce the plastic strain rate of the sample.

$$\dot{\varepsilon}_{plastic} = \dot{\varepsilon}_{total} - \frac{1}{E_{sample}}\left(\dot{\sigma}_{sample}\right) - \frac{1}{L_t} S \left(\frac{\partial F}{\partial t}\right) \quad (1)$$

where,

$\dot{\varepsilon}_{plastic}$ = plastic strain rate of sample [s^{-1}]
$\dot{\varepsilon}_{total}$ = total strain rate measured by LVDT_2 [s^{-1}]
E_{sample} = Young's modulus of sample [MPa]
$\dot{\sigma}_{sample}$ = sample stress relaxation rate [$MPas^{-1}$]
L_t = instantaneous length of sample [m]
S = machine stiffness correction constant [mN^{-1}]
$\left(\frac{\partial F}{\partial t}\right)$ = rate of change of force [Ns^{-1}]

The second term of Equation 1 contains the Young's modulus *E* of the sample material. Unfortunately, its value for bischofite and carnallite is not reported in literature. We thus

Table 1. Elastic modulus of the specimens

Sample	ρ [kg m^{-3}]	V_p [m s^{-1}]	V_s [m s^{-1}]	*N*	*G* [GPa]	*E* [GPa]
Carnallite	1600*	3938	1988	0.33	6.3	16.8
Bischofite	1600*	4312	2037	0.36	6.6	18.0
Mixture	1600*	3970	2207	0.28	7.8	19.8
Halite	2100*	--	--	--	--	39*

ρ: density of the material
V_p: longitudinal component of velocity (measured)
Vs: shear component of velocity (measured)
v: Poisson's ratio (calculated)
G: shear modulus (calculated)
E: Young's modulus (calculated)
*From literature

Determined these values for the material tested, by performing ultra-sonic time of flight sound velocity measurements on unconfined samples of bischofite, carnallite and the mixture under study, using the facilities at Technical University Delft (see Table 1).

3 Results

3.1 Mechanical data

The mechanical testing was done on a total of ten samples including three samples of bischofite, five samples of carnallite and two samples of their mixture with halite. The differential stress vs natural strain and time are plotted in Figure 1. The relaxation behaviour of all the salts was found to be nearly same so only three representative plots (bischofite5, carnallite2 and mixture1) of differential stress vs time are given here. The mechanical results of bischofite, carnallite and mixture samples, along with the experimental conditions have been tabulated in Table 2, where the differential stress values obtained at the end of each step are given. Since the main aim of this study is to produce a flow law to be applied at *in situ* conditions, we will assess how the obtained mechanical data fit to conventional power laws (Van Eekelen et al. 1984; Urai 1983; Ter Heege et al. 2005b), describing grain size insensitive (GSI – dislocation) creep and/or grain size sensitive (GSS – diffusion/pressure solution) creep, as given below

GSI: $$\dot{\varepsilon} = A^{*}\sigma^{n} \quad (2)$$

GSS: $$\dot{\varepsilon} = B^{*}\sigma d^{-p} \quad (3)$$

where $\dot{\varepsilon}$ is the strain rate, A^{*} is a substituted constant term for $A\exp(-Q/RT)$, where A is constant (for constant temperature), Q is the activation energy, R is the gas constant, T is the absolute temperature, B^{*} is also constant at a given temperature T, σ is the flow stress of the sample, n is the stress exponent, d is the average grain diameter, p is the grain size exponent.

3.1.1 Flow behaviour

All stress values obtained at the ends of the constant strain rate steps (Table 2), approaching steady state, are plotted against corresponding deformation strain rates in Figure 2a. Note that the dependent variable (stress) is plotted along the x-axis in this figure, to allow easier comparison with the relaxation data presented below. For bischofite, the best fit linear

Table 2: Test conditions and results of constant deformation parts

Test sample	$\dot{\varepsilon}$ [s^{-1}]	σ [MPa]	Experiment duration [days]	Test sample	$\dot{\varepsilon}$ [s^{-1}]	σ [MPa]	Experiment duration [days]
Bischofite5	10^{-5}	5.3	24	Carnallite1	10^{-5}	20.8	44
	10^{-6}	3.8			10^{-6}	13.2	
	10^{-7}	2.3			10^{-7}	9.0	
	10^{-8}	1.2			10^{-8}	5.5	
	10^{-7}	2.2			10^{-7}	9.0	
	10^{-6}	3.4			10^{-6}	14.0	
	10^{-5}	5.0			10^{-5}	24	
Bischofite6	10^{-6}	3.2	21	Carnallite2	10^{-5}	21.5	40
	10^{-6}	3.8			10^{-6}	13.4	
	10^{-5}	5.7			10^{-7}	9.0	
	10^{-5}	5.5			10^{-8}	5.2	
	10^{-7}	2.3			10^{-7}	9.0	
Bischofite7	10^{-5}	5.2	56		10^{-6}	14.5	
	10^{-6}	3.4			10^{-5}	24.3	
	10^{-7}	2.1		Carnallite3	10^{-5}	28.1	3
	10^{-8}	1.2			10^{-6}	18.8	
	10^{-7}	2.0			10^{-7}	11.1	

	10^{-6}	3.5		Carnallite4	10^{-5}	17.4	6
	10^{-5}	5.3		Carnallite5	10^{-5}	21.9	24
	10^{-6}	3.5			10^{-6}	13.8	
	10^{-6}	3.5			10^{-7}	9.4	
	10^{-5}	5.5			10^{-8}	6.1	
	10^{-5}	5.3			10^{-7}	10.2	
					10^{-6}	15.2	
					10^{-5}	23.8	
Mixture1	10^{-5}	25.7	42	Mixture2	10^{-5}	24.9	25
	10^{-6}	26.1			10^{-6}	21.6	
	10^{-7}	23.2			10^{-7}	16.8	
	10^{-8}	20.6			10^{-8}	10.8	
	10^{-7}	23.3			10^{-7}	16.7	
	10^{-6}	27.7			10^{-6}	21.1	
	10^{-5}	33.3			10^{-5}	25.2	

$\dot{\varepsilon}$ is the deformation strain rate
σ is the differential stress value at the end of the deformation step

regression (in log-log-space) resulted in n = 4.8±0.2 when applying the conventional power law of Equation (2). The steady state stress values have also been used to calculate n-values (cf. Eq. 2) for every individual step in strain rate of experiments bischofite5-6-7. The resulting values are plotted in Figure 2b. The n-value changes from about 6 at the higher stress to about 4 at the lower end of the stress range. This shows that a simple power law of the type of Equation (2) might not be applicable to the full data set for bischofite.

Five carnallite samples were tested and their stresses vs. natural strain data (Table 2) are shown in Figure 1b. Carnallite1 and 2 were both 7-step strain-rate stepping tests with three relaxation periods after constant strain rate deformation steps at 10^{-6}, 10^{-8} and 10^{-6} s^{-1},

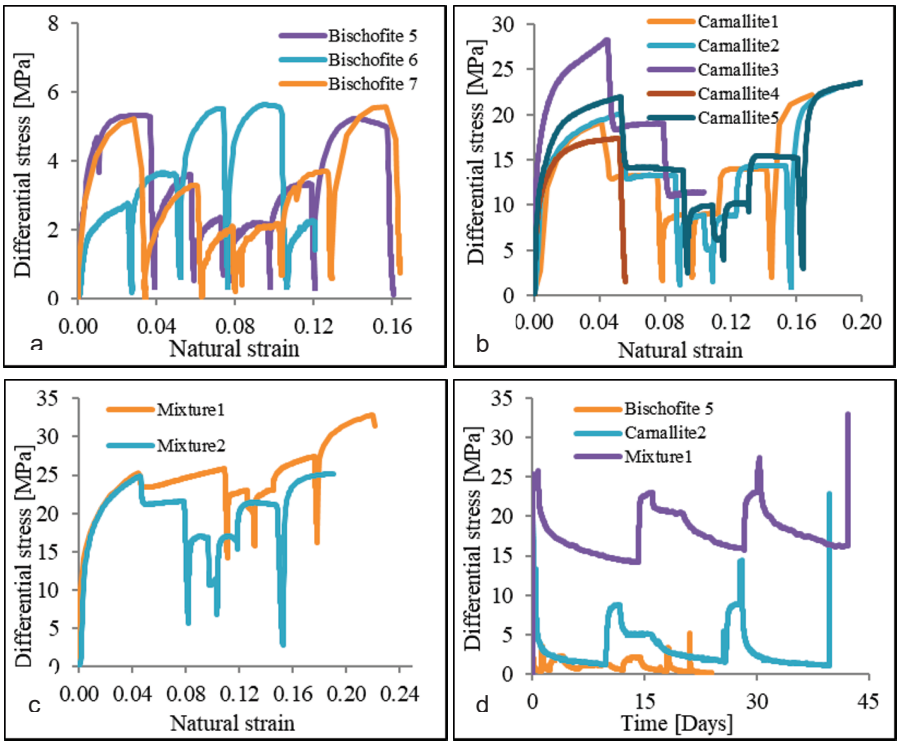

Figure 1. Mechanical data; differential stress vs. natural/true strain for bischofite (a), carnallite (b) and mixtures (c), and differential stress vs. time for three representative samples (d)

respectively. Carnallite3 was a 3-step stepping test without relaxation, carnallite4 was a single step deformation test followed by stress relaxation, and carnallite5 was a repeat experiment of carnallite 1 and 2. The samples showed strain rate sensitivity of stress, and strengths at the end of similar (repeat) strain rates were slightly higher for steps at higher total strains (see Table 2). The strengths of carnallite1, 2 and 5 are in good agreement with each other, demonstrating good reproducibility. Carnallite3 was comparatively too strong when compared with carnallite1, 2 and 5 at similar strain rates, while carnallite4 was found to be slightly weaker than the other samples. All stress values obtained at the end of the constant strain rate steps (Table 2), approaching steady state, are plotted against strain rate in Figure 2a. Best fit linear regression (in log-log-space, Fig. 2b) resulted in n = 5.1 ±0.3 when applying the conventional power law of Equation (2).

Two multistep experiments were performed on mixed bischofite-carnallite-halite samples. Mixture1 was a 7-step strain-rate stepping test with three relaxation periods after constant strain rate steps at 10^{-6}, 10^{-8} and 10^{-6} s^{-1}, respectively (see Table 2). The sample showed strain hardening in all constant strain rate steps, except for the one at the lowest rate. Mixture2 was also a 7-step strain-rate stepping test with three relaxation periods (Table 2), following the same sequence of steps as applied in mixture1. Mixture 2 was found to be weaker than mixture 1, and did not show the strain hardening as observed in mixture 1, but rather approached steady state stress behaviour in individual steps (Figure 1c). At the end of the

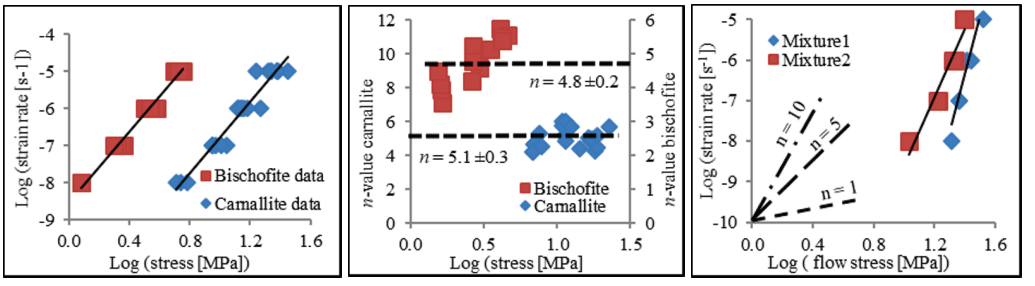

(a) (b) (c)

Figure 2. a) Steady state stress values of bischofite and carnallite samples against the strain rate on log space, b) n-value at different steady state stress values in bischofite and carnallite, c) n-value at different steady state stress values in mixture

experiment, the sample was taken out of the testing machine and localized strain along the pre-existing carnallite band was observed. This localized shear strain at the carnallite band most probably caused some leakage of the rubber jacket in the final stage of the experiment, which allowed some silicone oil to effuse through jacket and contaminate the sample. The sensitivity of stress to strain rate of the two mixtures is illustrated in Figure 2c, plotting the stress values at the end of each step as a function of strain rate, again with strain rate along the y-axis. The Figure 2c quite clearly illustrates the hardening behaviour of mixture1 and shows that the sensitivity of the differential stress to strain rate is rather low (high n-value), whereas the flow behaviour of mixture2 does not follow a linear trend in log-log space. Expressed using the power law n-value (Eq. 2), the trend is from n ~ 10 at the higher stress and faster strain rate, to n ~ 5 at lower stress and slower strain rate.

3.1.2 Stress relaxation

The stress relaxation results obtained are plotted in Figures 3a-c. The steady state stress values obtained at the end of each strain rate step are included in the graphs and form the starting points for relaxation. Moreover, the relaxation behaviour of all samples appeared identical and we have selected only three representative curves i.e. bischofite5, carnallite2 and

mixture1. Results at similar strain rate are combined. Generally, the graphs of bischofite and carnallite show that the evaluated plastic strain rate at the start of each relaxation fit to a trend with relatively high *n*-value ($n \sim 5$), implying that stress is relatively insensitive to strain rate. During relaxation then, the stress-strain rate sensitivity gradually increases and the *n*-value appears to approach $n = 1$ near the end of each relaxation step. Strikingly, the individual relaxation curves, starting at a particular strain rate and gradually decreasing in strain rate, do not pass through the steady state values obtained during the constant strain rate parts at lower rates. If compared at the same strain rate, the strength of the material during relaxation is always less than that during the constant strain rate part.

The stress relaxation data of mixtures are shown in Figure 3c. The steady state values obtained at the end of each deformation step are included in the graphs and from the starting points of relaxation. For comparison, similar strain rate steps are combined. At start of relaxation, the *n*-value is high ($n > 10$) showing steep slope, implying that the stress is relatively insensitive to strain rate. During relaxation then, the *n*-value decreases and appears to approach $n = 1$ near the end of each relaxation step. Distinctly, mixture1 relaxation curve progressively, passes through the steady state points obtained during deformation steps, pointing that the mixture2 shows weaker behaviour during relaxation than during deformation.

4 Discussion

4.1 Mechanical behaviour

The stress strain plots of the three salts tested; Figures 1(a-c), showed that these materials have different strengths for similar strain rates and temperature. Bischofite was found the weakest in the series. Carnallite appeared stronger than bischofite and the mixture was found even stronger than carnallite. If we compare our work with previous studies on halite by Heard (1972), Wawersik & Zeuch (1986), Carter (1993) and Ter Heege et al. (2005a), we see (Figure 4a) that the upper limit (highest stress at a given strain rate) is constrained by the flow law by Heard (1972 - confined tests on polycrystalline natural halite aggregates) at the temperature of 70 °C. Carnallite is weaker and lies around the flow law given by Wawersik & Zeuch (1986), whereas the bischofite is clearly the weaker end in the family. The data set on the mixtures is not extensive enough to allow a meaningful definition of the creep behaviour in terms of GSS creep cf. Equation (3).

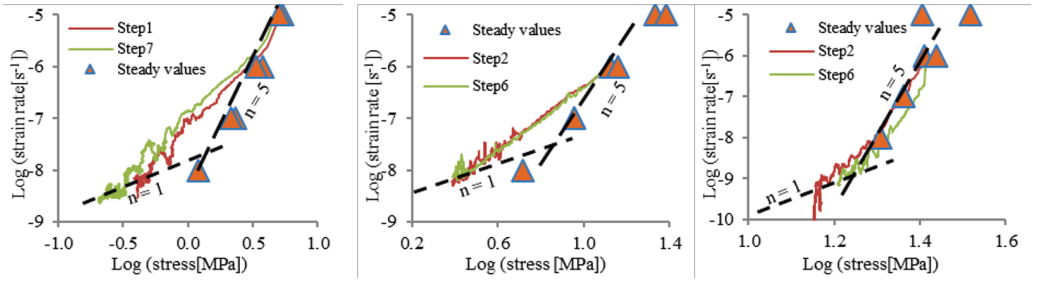

Figure 3. Stress relaxation curves a) bischofite5, step1 and step7 $\dot{\varepsilon} = 10^{-5}$ s^{-1}, b) carnallite2, step2 and step6 $\dot{\varepsilon} = 10^{-6}$ s^{-1}, c) mixture1 step2 and step6 $\dot{\varepsilon} = 10^{-6}$ s^{-1}

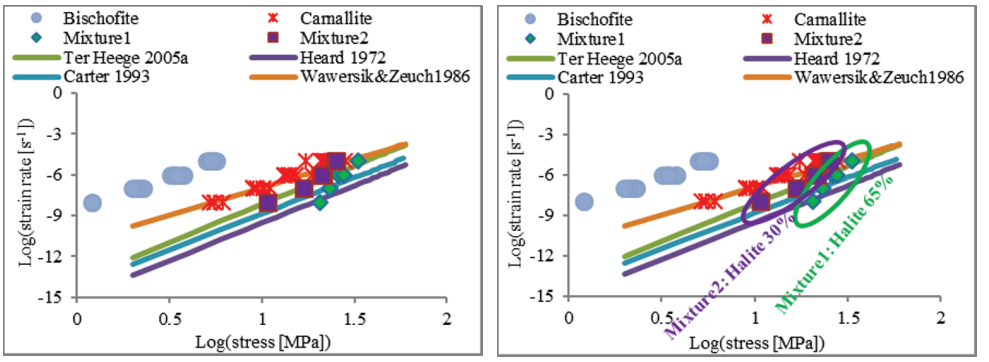

(a) (b)

Figure 4 a) Projected curves for flow laws of wet halite from previous studies, b) steady state values comparison of bischofite, carnallite and mixture (with halite% composition)

4.2 Composite flow law

The basis for determining composite flow laws were the data obtained during the deformation at constant strain rates, providing near steady state stresses, and the analysis of the relaxation curves under the assumption of constant structure. We will now evaluate if combining GSI and GSS creep in the form of a composite creep law is of added value. We start from:

$$\dot{\varepsilon} = A^*\sigma^n + B^*\sigma d^{-p} \quad (4)$$

Since our study did not systematically involve experiments on materials with different grain sizes, we explore the possible role of GSS creep using predictions on the basis of recrystallized grain size piezometers for the salts under consideration. In a recrystallized grain size piezometer, the size of the grains is directly related to the differential stress (e.g. Twiss 1977, Shimizu 2008, De Bresser et al. 2001) according to:

$$d = K\sigma^{-m} \quad (5)$$

where *K* and *m* are material and mechanism specific constants.

Van Eekelen et al. (1981) measured the recrystallized grain size in a number of bischofite samples experimentally deformed at 60 °C. We used their data to calibrate the values for *K* and *m* in Equations (5) and (4.11) by simply applying

$$d = K(\sigma)^{-1/slope} \quad (6)$$

The resulting piezometric relation for bischofite (with d in mm) is:

$$d = 4.725\sigma^{-1.15} \quad (7)$$

Using the piezometer of Equation (7), we can now estimate the recrystallized grain size at any stress, under the assumption the dynamic recrystallization was fully effective at the conditions imposed. We have done this for the average stresses relevant for our bischofite samples at the start of the relaxation periods, after steps at constant strain rate of 10^{-5}, 10^{-6}, 10^{-7} and 10^{-8} s^{-1}. The role of grain size can now be further evaluated by; i) assuming that during relaxation the grain sizes will remain the same, ii) and that a GSS creep law of the type of Equation (3), with *n* = 1, applies at the final stages of relaxation, i.e. at the very slow strain

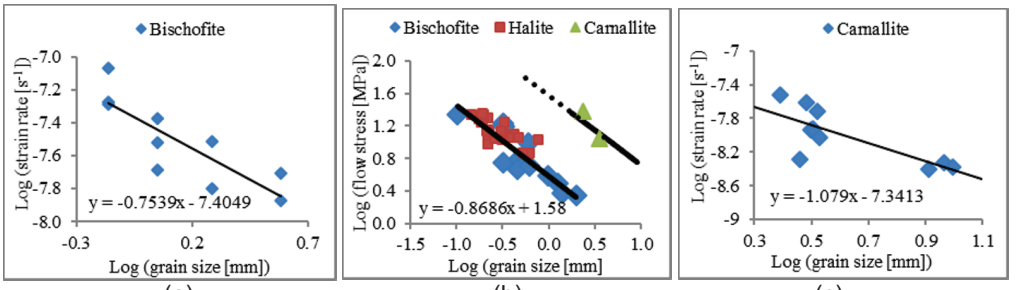

Figure 5. a) Bischofite Log strain rate values picked from relaxation curves at similar stress of 1.0 MPa, b) carnallite measured grain sizes in log space with halite and bischofite, c) strain rate values picked from relaxation data plotted against stress equivalent grain size from piezometer

rates. This allows calculating the *p*-value (Equation 3). Taking logarithm and simplifying the Equation (3) we get

$$log\dot{\varepsilon} = intercept - plogd \tag{8}$$

The intercept includes the stress and is only a constant if data are considered at single value of stress. For this, we picked σ = 1.0 MPa (i.e. Logσ = 0) in the stress relaxation curves (Figure 3a), determined the strain rate values at the various relaxation curves, and plotted the results, in log-log space (cf. Eq. 8, see Fig. 5a), against the evaluated grain sizes. Then using Equation (8), the grain size exponent '*p*' can be determined as from the slope of the best fit line (Figure 5a). As is clear from the Figure 5a, the scatter is quite substantial, so the resulting value for *p*, 0.8 ±0.2, must be regarded as only a crude estimate. Nevertheless, the result confirms the suggestion that grain size sensitive behaviour is likely to play a role in the flow behaviour of bischofite, at least during the relaxation.

A possible mechanism controlling flow in this GSS regime is dissolution or precipitation-controlled pressure solution creep (e.g. Spiers et al. 1990, Schutjens 1991). According to these studies, the inter-granular pressure solution creep (IPS) is a serial process comprising of three steps; dissolution of material at high stress zones, transportation via diffusion to lower stress zones and precipitation at low stress zones. The slowest of these will determine the creep rate. The creep rate is inversely related to the grain size ('d^{-p}'), where *p* = 1 and 3 are the sensitivities of the rate controlling mechanism to grain size, defining interface dissolution/precipitation and diffusion respectively.

Using the intercept value of the best fit line (Fig. 5a), the unknown constant *B** of Equation (3) was calculated to be 3.94×10^{-8} (MPa^{-1} $mm^{0.8}$ s^{-1}). Hence, the GSS flow law for bischofite at 70 °C, with grain size *d* in mm, is

$$\dot{\varepsilon}_{GSS} = 3.94 \times 10^{-8} \sigma d^{-0.8} \tag{9}$$

No recrystallized grain size piezometric relation is available in the literature for carnallite. We plotted our grain size data of two carnallite samples as a function of stress together with the data for halite (Ter Heege et al. 2005b) and bischofite (Van Eekelen et al. 1981) in Figure 5b. Bischofite and halite follow very comparable trends, but the grain size of carnallite at a given stress is substantially larger than that of halite and bischofite. We assumed that the trend observed for halite and bischofite also holds for carnallite, coming from the same family of materials. We thus suggest that the recrystallized grain size Piezometric relation for carnallite (Fig. 5b) is:

$$d = 65.92\sigma^{-1.15} \tag{10}$$

Now doing the same exercise for carnallite as carried out for bischofite, applying Equations (3) and (8) under the assumption of constant structure (grain size) during relaxation, we can obtain a crude estimate for the *p*-value for carnallite. We picked σ = 4.0 MPa (i.e. Logσ = 0.6) in the

stress relaxation curves (Figure 5b), determined the strain rate values at the various relaxation curves, and plotted the results, in log-log space against the values for the grain size,

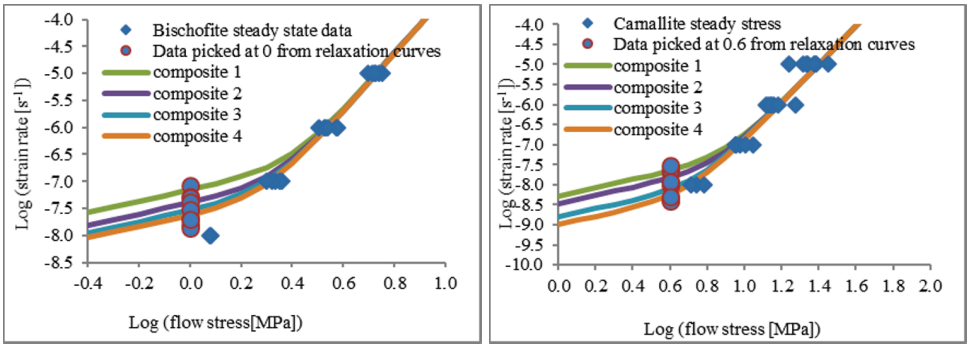

(a) (b)

Figure 6. Trends resulting from the composite GSI + GSS flow law covering the steady state behaviour (diamond data points) as well as the gradual decrease in *n*-value during relaxation (from $n \sim 5$ to $n \sim 1$ when going towards low stress and strain rate), a) bischofite, b) carnallite

see Figure 5c. The resulting value for *p* was: 1.0 ±0.26. Using the intercept value of the best fit line (Figure 5c), the unknown constant B^* of Equation (3) was calculated to be 1.01×10^{-8} (MPa^{-1} $mm^{1.0}$ s^{-1}). Hence, the GSS flow law for bischofite at 70 °C, with grain size *d* in mm is

$$\dot{\varepsilon}_{GSS} = 1.01 \times 10^{-8} \sigma d^{-1.0} \tag{11}$$

Equation (4), however, cannot simply be regarded as the sum of the GSI and GSS creep laws defined separately, since grain size sensitive behaviour might have influenced the steady state creep while this was not considered in performing the best fitting exercise. In other words, the established GSI creep law might not hold for the complete stress – strain rate range covered. We assume now that at the highest stress, GSI creep is robust. Regression analysis taking only the data into account at strain rate 10^{-6} and 10^{-5} s^{-1}, i.e. at the higher stresses, then results in $n = 5.4\pm0.4$ for bischofite and $n = 5.3\pm0.7$ for carnallite. Using these new values for the stress exponent *n*, holding for the GSI part of the composite Equation (4), and taking the established GSS flow equations, non-linear regression best fitting resulted in values for A^* of Equation (4).

For bischofite:

$$\dot{\varepsilon} = 1.1 \times 10^{-9} \sigma^{5.4} + 3.94 \times 10^{-8} \sigma d^{-0.8} \tag{12}$$

For carnallite:

$$\dot{\varepsilon} = 3.70 \times 10^{-13} \sigma^{5.3} + 1.01 \times 10^{-8} \sigma d^{-1} \tag{13}$$

The trends representing composite flow for bischofite: (for a grain size of 0.5 mm (composite1), 1.0 mm (composite 2), 1.5 mm (composite 3) and 2.0 mm (composite 4)) and carnallite: (for a grain size of 2 mm (composite1), 3 mm (composite 2), 6 mm (composite 3) and 9 mm (composite 4)) following Equations (12) and (13) are shown in Figures (6a-b).

The trend lines in Figures (6a-b) show that the influence of grain size is effective at lower stresses and strain rates. For higher stresses, these curves satisfy the steady state points, whereas on lower stress/strain rates, these trends satisfy the data picked from relaxation curves. Hence, the composite flow laws give a complete picture of the creep characteristics of bischofite and carnallite, in two regimes of GSI ($n \sim 5$) and GSS ($n \sim 1$) that gradually pass into each other.

Conclusions

Deformation experiments were conducted on bischofite, carnallite and mixed bischofite-carnallite-halite samples obtained from natural cores. Main aim was to produce constitutive flow laws that can be applied at *in situ* conditions. The experiments were carried out at a confining pressure of 40 MPa and a temperature of 70 ºC. The experiments were multi-step tests consisting of constant strain rate parts and stress relaxation parts. The flow laws developed are mainly on the basis of mechanical data, microstructural work is for future.

The main findings are:

1. Carnallite is 4-5 times stronger than bischofite. The bischofite-carnallite-halite mixtures, at their turn, are stronger than carnallite, and hence also stronger than bischofite. We infer that the difference in strength from one mixture to the next is best explained by differences in halite wt. %.
2. The constant strain rate parts of the multistep experiments allowed defining (dislocation/grain size insensitive GSI) creep laws for bischofite and carnallite.
3. For bischofite as well as carnallite, we observed that during stress relaxation, the conventional power law stress exponent in the creep laws changes from ~5 at 10^{-5} to ~1 at 10^{-9} s^{-1}. This is interpreted as reflecting a change from grain size insensitive (GSI) dislocation creep at the faster strain rates to grain size sensitive (GSS) behaviour at slow strain rate.
4. If during deformation of bischofite and carnallite the microstructure is continuously being reworked, some balance might develop between the GSI and GSS mechanisms, at the boundary between the creep regimes. The established single GSI flow laws then form solid descriptions of the creep behaviour of these materials. In cases that effective microstructural modification cannot be assumed, as for example during transient creep in the walls of salt caverns, the composite creep laws form better descriptions.

Acknowledgements

This work was supported through a scholarship for NM awarded by the Higher Education Commission of Pakistan and through additional sponsorship provided independently by AkzoNobel, Nedmag Industries and the Nuclear Research and Consultancy Group NRG. The authors thank Gert Kastelein, Peter van Krieken and Eimert de Graaff for technical support.

References

CARTER, N.L., HORSEMAN, S.T., RUSSELL, J.E. & HANDIN, J. 1993. Rheology of rocksalt. Journal of Structural Geology, 15 (9-10), 1257-1271.

CHRISTOV, C. 2009. Isopiestic Determination of the Osmotic Coefficients of an Aqueous $MgCl_2$ + $CaCl_2$ Mixed Solution at (25 and 50) °C. Chemical Equilibrium Model of Solution Behavior and Solubility in the $MgCl_2$ + H_2O and $MgCl_2$ + $CaCl_2$ + H_2O Systems to High Concentration at (25 and 50) °C J. Chem. Eng. Data, 54, 627–635.

DE BRESSER, J.H.P., TER HEEGE, J.H. & SPIERS, C.J. 2001. Grain size reduction by dynamic recrystallization: can it result in major rheological weakening?. International Journal of Earth Sciences, 90(1), 28-45.

HEARD, H.C. 1972. Steady-State Flow in Polycrystalline Halite at Pressure of 2 Kilo bars. Flow and Fracture of Rocks, 191-209.

HEARD, H.C. & RYERSON, F.J. 1986. Effect of Cation Impurities on Steady-State Flow of Salt,Mineral and Rock Deformation: Laboratory Studies: The Paterson Volume, 99-115.

JACKSON, M.P.A. & TALBOT, C.J. 1986. External shapes, strain rates, and dynamics of salt structures. Geological Society of America Bulletin 97.3: 305-323.

MUHAMMAD, N. 2015. Deformation and transport processes in salt rocks: An experimental study exploring effects of pressure and stress relaxation. Utrecht Studies in Earth Sciences, 84, 1-275.

MUHAMMAD, N., SPIERS, C.J., PEACH, C.J. & DE BRESSER, J.H.P. 2012. Effect of confining pressure on plastic flow of salt at 125 ºC. In: Bérest, P., Ghoreychi, M., Hadj-Hassen, F., and Tijani, M. eds. Mechanical behaviour of salt VII, CRC press, 57-64.

ROEDDER, E. & BASSETT, R.L. 1981. Problems in determination of the water content of rock-salt samples and its significance in nuclear-waste storage siting. Geology 9, no. 11: 525-530.

RUTTER, E.H. & MAINPRICE, D.H. 1978. The effect of water on stress relaxation of faulted and unfaulted sandstone. Pure and Applied geophysics 116.4-5: 634-654.

SCHUTJENS, P.M.T.M. 1991. Intergranular pressure solution in halite aggregates and quartz sands: an experimental investigation. Geologica Ultraiectina, 76, 1-233.

SHIMIZU, I. 2008. Theories and applicability of grain size piezometers: The role of dynamic recrystallization mechanisms. J. Struct. Geol. 30, 899-917.

SPIERS, C.J., SCHUTJENS, P.M.T.M., BRZESOWSKY, R.H., PEACH, C.J., LIEZENBERG, J.L. & H.J. ZWART, H.J. 1990. Experimental determination of constitutive parameters governing creep of rocksalt by pressure solution. Geological Society, London, Special Publications 54, no. 1: 215-227.

SPIERS, C.J. & CARTER, N.L. 1998. Microphysics of Rocksalt Flow in Nature, The Mechanical Behaviour of Salt IV. Proceedings of the Fourth Conference. M. Aubertin,H. R. Hardy Jr., Trans. Tech., Clausthal-Zellerfeld, Germany, 115–128.

TER HEEGE, J.H., DE BRESSER, J.H.P. & SPIERS, C.J. 2005a. Rheological behaviour of synthetic rocksalt: The interplay between water, dynamic recrystallization and deformation mechanisms. J. Struct. Geol. 27, 948-963.

TER HEEGE, J.H., DE BRESSER, J.H.P. & SPIERS, C.J. 2005b. Dynamic recrystallization of wet synthetic polycrystalline halite: dependence of grain size distribution on flow stress, temperature and strain," Tectonophysics 396.1: 35-57.

TWISS, R.J. 1977. Theory and applicability of a recrystallized grain size paleopiezometer. Pure and applied Geophysics 115, 227-244.

URAI, J.L. 1983. Water assisted dynamic recrystallization and weakening in polycrystalline bischofite. Tectonophysics 96.1: 125-157.

URAI, J.L. 1985. Water-enhanced dynamic recrystallization and solution transfer in experimentally deformed carnallite. Tectonophysics, 120(3), 285-317.

URAI, J.L., SPIERS, C.J., ZWART, H.J. & LISTER, G.S. 1986. Weakening of rock salt by water during long-term creep. Nature 324, 554–557.

VAN EEKELEN, H.A., URAI, J.L. & HULSEBOS, T. 1981. Creep of bischofite. In Prodeedings of the 1st Conference on the Mechanical Behavior of Salt, Pennsylvania, USA. Trans. Tech., Clausthal-Zellerfeld, Germany.

WAWERSIK, W.R. & ZEUCH, D.H. 1986. Modeling and mechanistic interpretation of creep of rock salt below 200 ºC. Tectonophysics, 121(2), 125-152.